

Computational Design of Inorganic Solid-State Electrolyte Materials for Lithium-Ion Batteries

Jiale Ma and Zhenyu Li*

Cite This: *Acc. Mater. Res.* 2024, 5, 523–532

Read Online

ACCESS |

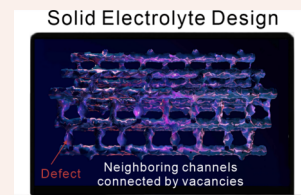
Metrics & More

Article Recommendations

Supporting Information

CONSPPECTUS: Solid-state electrolytes hold great promise for advancing electrochemical energy storage devices. Advanced batteries based on solid electrolytes, particularly all-solid-state lithium-metal batteries, hold the potential to simultaneously address both high energy density and safety concerns associated with traditional lithium-ion batteries. Ideally, solid electrolytes should exhibit a high ionic conductivity at room temperature. In practical applications, other properties, such as electrochemical stability and compatibility with electrodes, are equally important. However, the pursuit of a single solid electrolyte possessing all of these properties remains challenging. Simulation techniques play an important role in the design of solid electrolyte materials, bypassing the difficulty of chemical synthesis and structural characterization. In these simulations, ionic conduction within bulk electrolytes and the ion deposition and stripping processes at the charged electrode–electrolyte interface can be investigated. By providing the flexibility to construct electrolyte models and explore structural evolution at multiple scales, simulation techniques facilitate the rational design of advanced solid electrolytes that maximizes their advantages and mitigates limitations. This account is initiated by introducing fundamental theories and simulation techniques to investigate the ionic conductivity of an inorganic solid electrolyte. Subsequently, we present our recent progress in designing high ionic conductivity electrolytes by increasing the concentration of Li vacancies, by tuning the type of defects, by constructing diffusion pathways, and by avoiding ion crowding. At last, the electrochemical stability of inorganic solid electrolytes and their compatibility with lithium-metal electrodes are addressed.

In bulk electrolytes, increasing the defect concentration can often enhance the ionic conductivity. For instance, to surpass the upper limit of Li vacancy concentration without compromising structural stability, we adopt an antispinels crystal structure, enhancing Li mobility within the Li_3OBr electrolyte. The type of defects also matters. Instead of O doping, we propose to introduce Li interstitials effectively through S doping, significantly reducing lattice distortion and eliminating the anchoring effect of Li around the O dopant. Compared to the electrolyte with vacancy defects, introducing Li interstitials boosts the ionic conductivity of Li_3OCl by 3 orders of magnitude. In addition to defect engineering, designing a three-dimensional diffusion pathway for Li ions enhances bulk ionic conductivity. While LaCl_3 -based electrolytes exhibit good compatibility with Li-metal electrodes, their intrinsic low ionic conductivity poses limitations. We propose constructing a three-dimensional diffusion pathway by connecting neighboring one-dimensional channels through the introduction of La vacancies, significantly enhancing the ionic conductivity of LaCl_3 -based electrolytes at room temperature. Furthermore, we investigate ion diffusion in the space charge layer (SCL) near charged solid interfaces. We observe that the mobility of Li interstitials in the SCL is close to that of Li vacancies in bulk electrolytes. However, a defect-deficient region within the SCL may induce high ionic resistance. These studies demonstrate that material design based on simulation techniques offers promise for the development of solid electrolytes and the advancement of electrochemical energy storage devices.



1. INTRODUCTION

Lithium-metal batteries (LMBs), using lithium metal as the anode material, have high theoretical capacities which is desirable for the fast-increasing demand for electronic vehicles and grid storage.^{1,2} However, the application of LMBs is limited by the severe safety issues induced by lithium dendrite growth and leakage of flammable liquid electrolyte. Solid electrolyte with high stiffness can effectively suppress the growth of Li dendrites, addressing the safety and energy density issues of conventional lithium-ion batteries.^{3–5} There are different types of solid-state electrolytes, including inorganic, polymer, and ceramic–polymer composite electrolytes.³ Polymer and ceramic-polymer composite electrolytes exhibit a unique combination of properties, including good

shape flexibility, good contact with electrodes, relatively narrow electrochemical window, and low ionic conductivity at room temperature. With the integration of a ceramic filler in the polymer host, composite polymer electrolytes help to increase the low ionic conductivity. Inorganic solid electrolytes usually have better electrochemical stability, thermal stability, and

Received: October 27, 2023

Revised: March 3, 2024

Accepted: March 4, 2024

Published: March 19, 2024



mechanic strength while having a wider range of ionic conductivity. They can be further categorized into several subgroups, each with its own advantages and drawbacks. For example, oxide solid electrolytes exhibit high electrochemical stability and ionic conductivity but suffer from poor electrode contact. Sulfide electrolytes offer high ionic conductivity and good mechanical flexibility, but the stability of the electrode/electrolyte interface is lacking. Halide electrolytes possess excellent compatibility with electrodes, yet they are sensitive to moisture. Hydride electrolytes present excellent mechanical properties but lack satisfactory chemical and thermal stability. Therefore, it is challenging to find a solid-state electrolyte which satisfies all necessary properties, including high ionic conductivity, wide electrochemical window, and good electrode/electrolyte compatibility.⁶ A rational design of solid electrolytes is thus important.

With the ability to direct exploration of ion migration in bulk electrolyte and Li deposition/stripping processes on the electrode/electrolyte interface at different length and time scales, theoretical simulation techniques emerge as important tools for the design of solid electrolyte material. Simulations also have the advantages of manipulating models precisely and freely without chemical synthesis or structure characterization. For example, the dependence of ionic conductivity of bulk electrolyte on defect concentration,^{7–9} correlation between ions,^{10,11} local crystal structure,^{9,12} and 3-dimensional architecture of the diffusion pathway^{6,13,14} can be simulated, which provides a comprehensive understanding of ion diffusion mechanism. Simulations can also be used to investigate the structure evolution at different scales. For example, the tendency of Li dendrite growth can be evaluated by the self-diffusion barrier of a Li ion on the electrode surface calculated with density functional theory at the atomistic scale.^{15,16} It can also be investigated by simulating the deposition of Li ions using molecular dynamics simulations at the nanoscale.^{17,18} Using continuum models, Li dendrite growth can be simulated at the microscale to directly compare with experimental observations.^{19,20} A multiscale understanding obtained from simulations is helpful in the design of solid electrolyte materials.

In this Account, we focus on the computational design of inorganic solid-state electrolytes. We first introduce theories and simulation techniques to estimate the ionic conductivity of an inorganic solid electrolyte. Then, we discuss recent progress on ionic conductivity enhancement via defect engineering and construction of 3D diffusion pathways. Moreover, Li mobility in a space charge layer (SCL) near the charged interface is discussed. At last, the simulations of electrochemical stability and compatibility between the electrode and electrolyte are addressed. These results demonstrate that simulation techniques can play an important role in the rational design of solid electrolyte materials.

2. COMPUTATIONAL INVESTIGATION OF IONIC CONDUCTIVITY OF SOLID ELECTROLYTES

A challenge in solid electrolyte applications is how to enhance their ionic conductivity. The atomic-level understanding of Li diffusion within crystalline materials is essential to the design of solid electrolyte materials with a high ionic conductivity. One possible way to characterize the Li mobility is to calculate the diffusion barrier E_b by searching the transition state of Li on a predetermined path based on structural optimization methods such as the nudged elastic band (NEB) method.²¹

The lower the diffusion barrier, the easier the Li hopping between different lattice sites. As shown in Figure 1, for the

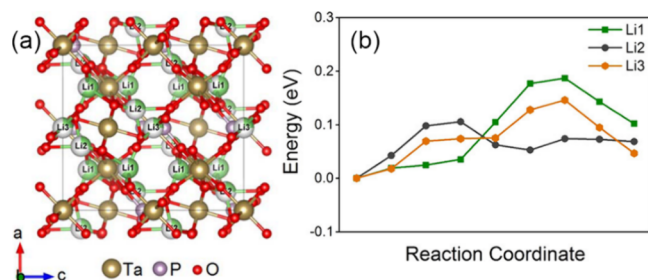


Figure 1. Diffusion barrier of Li in LiTa_2PO_8 . (a) Crystal structure of LiTa_2PO_8 . Different Li sites are marked with Li1, Li2, and Li3. (b) Energy profile of Li diffusion along different pathways. Reproduced with permission from ref 22. Copyright 2019 American Chemical Society.

inorganic solid electrolyte LiTa_2PO_8 , the barriers for Li diffusion among neighboring vacancies can be predicted for three different paths. Such a method is effective if the diffusion behavior is determined by a certain number of dominant diffusion pathways. However, this is not always the case, especially when the structure of the environments becomes complex and the temperature becomes high.^{22,23}

Another choice to investigate the ion mobility without relying on specific pathways is to directly simulate the diffusion of Li in solid electrolyte via molecular dynamics (MD) simulations. Then, the diffusion coefficient of atoms or ions in solid electrolyte can be obtained by calculating the mean square displacement (MSD) as a function of time:

$$D = \lim_{t \rightarrow \infty} \left[\frac{1}{2dt} \langle [\vec{r}(t)^2] \rangle \right] \quad (1)$$

where d is the dimension of the diffusion system. MSD is calculated via a sampling of the MD trajectory

$$\langle [\vec{r}(t)]^2 \rangle = \frac{1}{N} \sum_{i=1}^N [\vec{r}_i(t_0 + t) - \vec{r}_i(t_0)]^2 \quad (2)$$

where N is the total number of the diffusing particles; $\vec{r}_i(t_0)$ is the position of the i th particle at time t_0 ; and $\vec{r}_i(t_0 + t)$ is the position of that particle at time t after t_0 . Notice that t_0 is a sampling variable, and there is an average over different t_0 which is not explicitly included on the right side of eq 2. In MD simulations, interatomic interactions can be described by either an empirical force field or more accurately by computationally expensive *ab initio* methods. Notice that the overall accuracy of diffusion properties predicted from MD simulations depends on not only the accuracy of the interatomic potential but also the quality of the sampling. *Ab initio* molecular dynamics (AIMD) simulation can accurately describe the interatomic interactions, but it is computationally expensive. Therefore, statistical convergence of the AIMD sampling should be checked.

As an example, MSDs for ions in the electrolyte material LiTa_2PO_8 are calculated. As shown in Figure 2, the MSD of Li ions increases with time, while those for other elements stay at values close to 0. These results indicate that Li ions indeed diffuse, while other atoms keep oscillating around their equilibrate positions. The Li MSD increases slower at lower temperatures, which makes the convergence of the diffusion

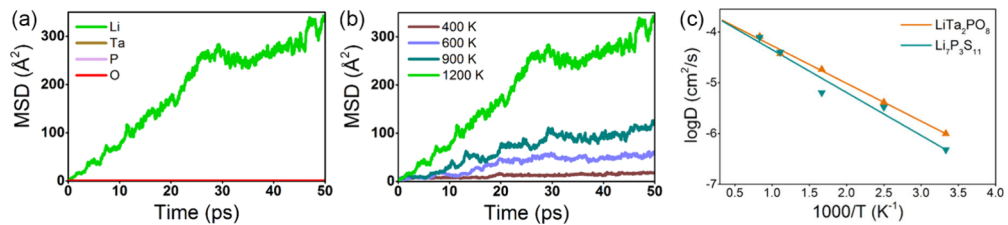


Figure 2. (a) Mean square displacement (MSD) for different elements in LiTa₂PO₈ at 1200 K. (b) MSD of Li in LiTa₂PO₈ at different temperatures. (c) Arrhenius plot of the Li diffusion coefficient in solid electrolytes LiTa₂PO₈ and Li₇P₃S₁₁. Reproduced with permission from ref 22. Copyright 2019 American Chemical Society.

coefficient more difficult at low temperature. Therefore, it is a common measure to predict the diffusion coefficient at room temperature via extrapolation from high temperatures

$$D = D_0 \exp\left(-\frac{E_a}{k_B T}\right) \quad (3)$$

where E_a is the activation energy; k_B is the Boltzmann constant; and T is the temperature. In most computational studies, the concentration of defects is set to be a predetermined parameter without considering the influence of temperature. As a result, the activation energy E_a from AIMD simulation is usually close to the diffusion barrier E_b calculated by searching the minimum energy path. For example, the E_b of three diffusion paths in LiTa₂PO₈ electrolyte are 0.19, 0.15, and 0.11 eV, respectively, while the E_a from the AIMD simulation is 0.16 eV.²² When comparing to the activation energy obtained in experiments at different temperature, the defect formation energy should be considered.²⁴

With the diffusion coefficient, ionic conductivity can be calculated using the Nernst–Einstein equation

$$\Lambda = \frac{\rho F^2 z^2}{RT} D \quad (4)$$

where ρ is the molar density of ions; F is the Faraday constant; z is the valence of the ion; and R is the gas constant. In the example of Li_{0.33}La_{0.56}TiO₃, the room-temperature ionic conductivity predicted from AIMD (1.906×10^{-3} S/cm)²⁶ is quite close to the experimental conductivity (1.0×10^{-3} S/cm).²⁷ However, for LiTa₂PO₈, the ionic conductivity predicted from AIMD is 35.3 mS/cm at 300 K, which is about 20 times larger than the experimental value (1.6 mS/cm).²⁵ Such a difference may be contributed by effects of grain boundary²⁷ and other defects in experiment.

3. DESIGN OF INORGANIC SOLID ELECTROLYTES WITH ENHANCED IONIC CONDUCTIVITY

Compared to liquid electrolytes, the main problems of solid electrolytes are low ionic conductivity and high interfacial resistance. The ion migration in the crystalline electrolyte can be tuned by the concentration and distribution of point defects, which are expected to change the diffusion barrier of Li ions. It is also possible to achieve high ionic conductivity with a good design of crystal lattice. At last, the SCL at charged solid/solid interfaces can also significantly influence ion transport.

3.1. Ionic Conductivity Enhancement via Point Defects

In solid electrolyte, Li-ion transport is generally realized via hopping between neighboring lattice sites. The existence of point defects, such as vacancy and interstitial, can accelerate the hopping of ions and thus enhance the ionic conductivity.

For example, the ionic conductivity of perovskite Li_{0.33}La_{0.56}TiO₃ is several orders of magnitude higher than that of Li_{0.5}La_{0.5}TiO₃ since the former contains more vacancies.^{9,46}

An interesting example about the effects of defects is Li-rich antiperovskite (AP) electrolyte Li₃OX (X = Br, Cl), which has a wide electrochemical window.⁴⁶ However, pristine Li₃OX without defects is not a good Li-ion conductor with an ionic conductivity of only about 10^{-7} S/cm at room temperature. The ionic conductivity can be significantly enhanced by increasing the concentration of the vacancy defect. In our AIMD simulation of Li₃OBr electrolyte, no diffusion event was observed in a pristine AP Li₃OBr system even at 1500 K. The MSD starts to increase slowly at 2000 K (Figure 3a). When a

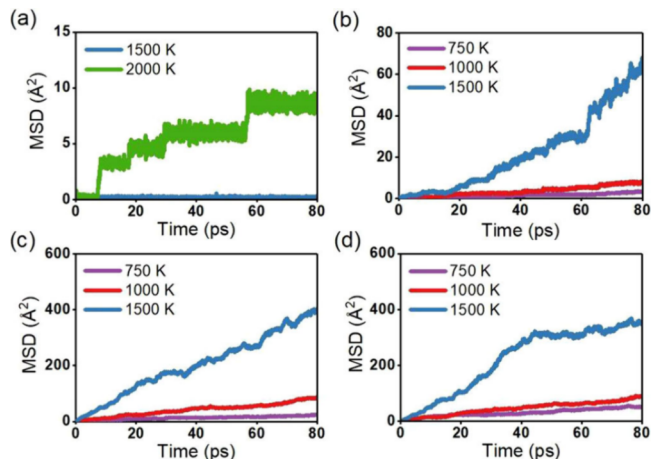


Figure 3. Mean square displacement of Li for (a) pristine AP Li₃OBr, (b) AP Li₃OBr with 12.5% LiBr vacancies, (c) AS Li₃OBr with intrinsic defects, and (d) AS Li₃OBr with an extra LiBr vacancy pair. Reproduced with permission from ref 7. Copyright 2018 Wiley.

pair of LiBr vacancies was introduced in the AP Li₃OBr system (1/24 Li vacancy), vacancy hopping was observed at 1000 K, and MSD started to increase at 1500 K (Figure 3b). Obviously, vacancies enhance Li diffusion in Li₃OBr. More specifically, Li vacancies enhanced the ionic conductivity since no Li ion was found to enter the Br vacancy site in the AIMD trajectory.

Unfortunately, the upward limit of vacancy concentration introduced by the depletion of LiBr is only 6.6% in the experiment. In contrast, a large number of intrinsic defects exist in Li₃OBr with an antispinell (AS) structure. At the same time, in contrast to the AP phase, anion vacancies in the AS phase are active, and Li ions can enter those sites. As a result, Li MSD increases significantly faster in the AS phase (Figure 3c) than that in the AP phase. The enhanced Li mobility can be visualized by plotting the Li-ion trajectories. As shown in

Figure 4, the Li trajectory is distributed over the whole cell in the AS phase, while it is limited around equilibrium sites in the AP phase.

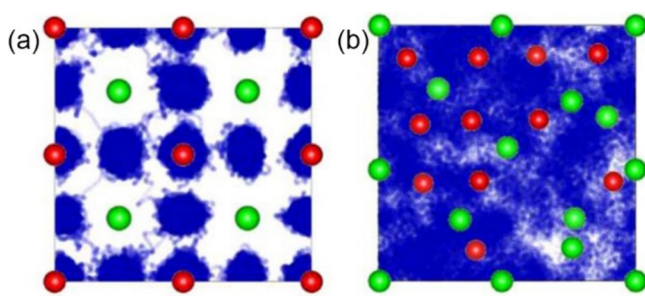


Figure 4. Li trajectory in (a) AP Li_3OBr with 12.5% vacancies and (b) AS Li_3OBr solid electrolyte at 1000 K. The trajectory of Li is colored in blue. O and Br atoms are colored in red and green, respectively. Reproduced with permission from ref 7. Copyright 2018 Wiley.

Effects of point defects on ionic conductivity also depend on the type of defects. Comparing to Li vacancies, Li interstitials in Li_3OCl associate with a much lower diffusion barrier (0.145 eV¹¹ vs 0.310 eV,¹¹ 0.367 eV⁴⁷). Thus, increasing the concentration of the Li interstitial should be a more effective way to enhance the ionic conductivity. To maintain the charge neutralization, the formation of an interstitial should be accompanied by an O substitution of Cl O'_{Cl} in the synthesis process of Li_3OCl . Here, we use the Kröger–Vink notation to indicate the charge statuses of defects, where negative, null, and positive charge statuses are represented by $'$, \times , and \bullet , respectively.⁴⁸

Unfortunately, the formation of a Li_i^{\bullet} and O'_{Cl} pair is thermodynamically unfavorable, and it is difficult to increase the concentration of Li interstitials. This is not strange considering the small radius of the amorphous sphere of O, which introduces a large lattice distortion when using the amorphous sphere of O to substitute Cl. At the same time, the large electronegativity enhances the electrostatic interaction between Li_i^{\bullet} around O'_{Cl} , which lowers the Li conductivity. To solve these problems, we propose a S-doping scheme, i.e., using S'_{Cl} to compensate the charge from Li_i^{\bullet} .

As shown in Table 1, with the doping of the S atom, the defect formation energy of the interstitial and substitution pair decreases from 1.68 eV ($\text{Li}_i^{\bullet} + \text{O}'_{\text{Cl}}$) to 1.14 eV ($\text{Li}_i^{\bullet} + \text{S}'_{\text{Cl}}$), which is even 0.26 eV smaller than the formation energy of the vacancy pair $\text{V}'_{\text{Li}} + \text{V}_{\text{Cl}}$. Furthermore, the binding energy between Li_i^{\bullet} and S'_{Cl} is decreased to a negligible value (-0.03 eV), and the distance between these two defects is increased. Therefore, the S-doping strategy makes the Li interstitial more energetically favorable and weakens the binding between Li and S substitution.

Table 1. Defect Formation Energy (E_f), Coulombic Binding Energy (E_{coul}), and Distance (l) between Defects in a Specific Defect Pair^a

	$\text{V}'_{\text{Li}} + \text{Li}_i^{\bullet}$	$\text{Li}_i^{\bullet} + \text{O}'_{\text{Cl}}$	$\text{Li}_i^{\bullet} + \text{S}'_{\text{Cl}}$	$\text{V}'_{\text{Li}} + \text{V}_{\text{Cl}}$	$\text{S}_{\text{O}}^{\times}$	$\text{V}_{\text{Li}}^{\times}$	Li_i^{\times}
E_f	2.002	1.676	1.141	1.398	1.353	3.778	3.026
E_{coul}	-0.004	-0.660	-0.031	-0.074			
l	2.90	1.78	4.43	4.77			

^aThe units of energy and distance are eV and Å, respectively. Reproduced with permission from reference 8. Copyright 2019 American Physical Society.

The Li mobilities in Li_3OCl with different defects are investigated. As shown in Figure 5, the diffusion barrier

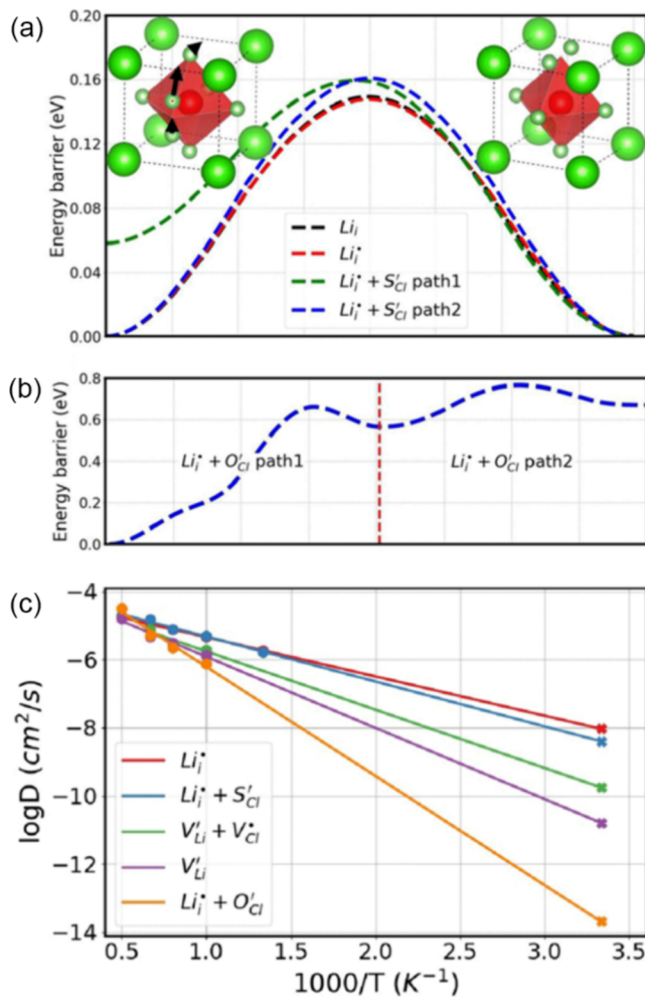


Figure 5. (a) Diffusion barrier of Li interstitial in pristine Li_3OCl and the S'_{Cl} system. (b) Diffusion barrier of Li interstitial in the O'_{Cl} system. (c) Arrhenius plot of the Li diffusion coefficient in systems with different defects. Reproduced with permission from reference 8. Copyright 2019 American Physical Society.

calculated with the NEB algorithm decreases from 0.66 eV ($\text{Li}_i^{\bullet} + \text{O}'_{\text{Cl}}$) to 0.15 eV ($\text{Li}_i^{\bullet} + \text{S}'_{\text{Cl}}$). This result indicates that the Li trapping center in the O'_{Cl} case disappears in the S doping case. As a result, the ionic conductivity of the Li interstitial is boosted from 3.82×10^{-4} to 1.29 mS/cm upon S doping. The enhanced ionic conductivity is around 20 times larger than the vacancy system ($5.70 \times 10^{-2} \text{ mS/cm}$). Therefore, defect engineering based on computational design provides a powerful tool for solid electrolyte development.

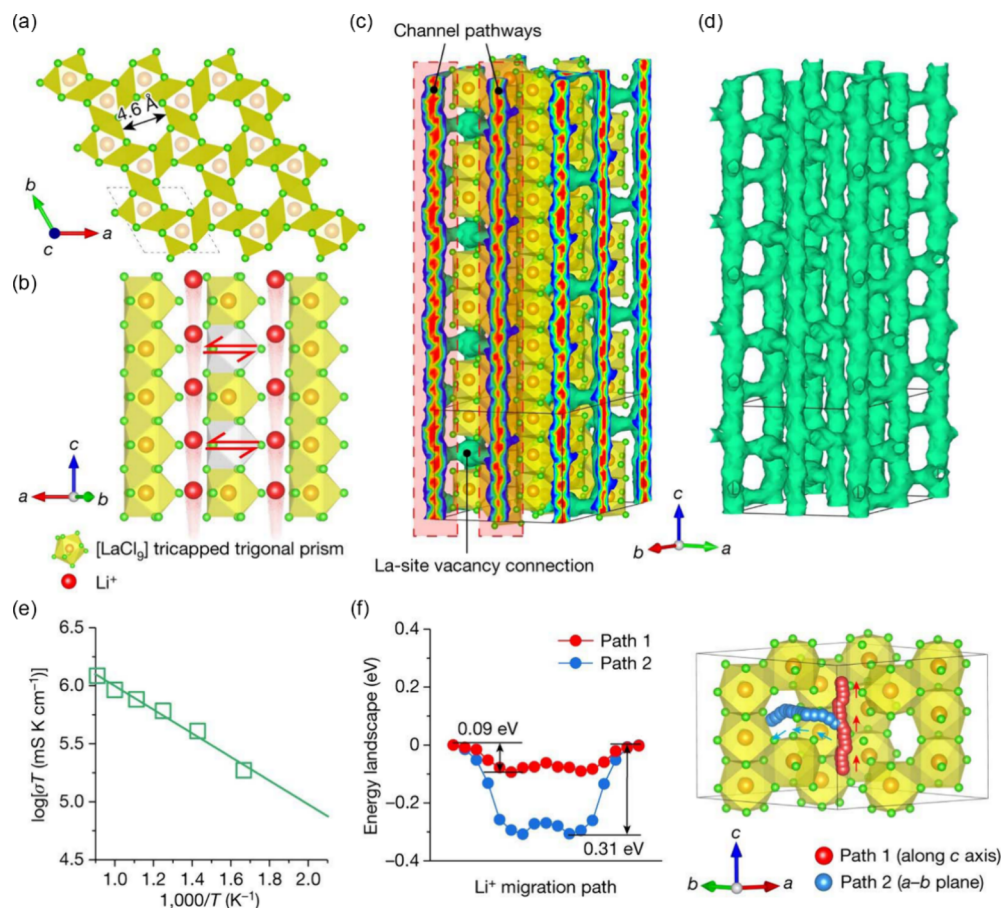


Figure 6. (a) Top view of the LaCl₃ lattice along the *c* axis. The inner diameter of 1D ion channels is 4.6 Å. (b) Side view of the vacancy-containing LaCl₃ lattice indicating Li migration along the 1D channel (red spheres) and between adjacent channels (bidirectional arrows). (c) Li probability density, represented by green isosurfaces from the AIMD simulation of LaCl₃ with vacancies at 900 K. (d) 3D diffusion pathway represented by isosurfaces of Li probability. Atoms are not shown for clarity. (e) Arrhenius plot of Li diffusion coefficients. (f) Li migration paths and the corresponding diffusion barrier. The red path represents the Li diffusion along the 1D channel, while the blue path represents the Li diffusion between adjacent channels through a La vacancy. Reproduced with permission from reference 6. Copyright 2023 Nature Publishing Group.

3.2. Ionic Conductivity Enhancement via Diffusion Channels

Diffusion channels can facilitate Li transport in solid electrolytes. Therefore, it is desirable to tune the topology and shape of the channels to enhance ionic conductivity. As an example, the energy barrier of Li diffusion in Li_{0.33}La_{0.56}TiO₃ corresponds to the transmission of ions through an O₄ bottleneck structure.⁹ Therefore, changing the bottleneck size can directly influence the hopping of ions. Besides local atomic structures, the overall diffusion pathway in the solid electrolyte can also be tuned to enhance ionic conductivity. Generally, a 3D continuous diffusion path is desirable for a fast ion transportation in crystalline solid electrolyte.^{10,13}

Halide electrolytes usually have a low ionic conductivity in the range of 10⁻⁸–10⁻⁵ S/cm.³ However, the excellent compatibility with lithium metal and good mechanical properties make them still important candidates for solid electrolytes. Increasing their ionic conductivity is thus the most important task for their practical applications. Recently, we found that the ionic conductivity of LaCl₃ can be enhanced via constructing 3D diffusion pathways.⁶ As shown in Figure 6a, the LaCl₃ lattice with the P6₃/m space group contains plentiful one-dimensional (1D) 4.6 Å channels enclosed by six columns of adjacent edge-sharing [LaCl₉] polyhedrons. 1D channels facilitate ion transport in specific directions. However, the

overall ionic conductivity turns out to still be low.¹³ We propose that 3D Li diffusion pathways can be constructed via connecting those parallel 1D ion channels through La vacancies (Figure 6b).

AIMD simulations are performed to investigate Li diffusion in Li₃La₅Cl₁₈. According to the Li probability distribution (Figure 6c), the 1D ion channel is fulfilled in the trajectory of Li, which is desirable for achieving rapid Li migration.⁴⁹ At the same time, with the existence of La vacancies, the 1D channels are connected with neighboring channels (Figure 6d), which construct an excellent 3D diffusion network.

Based on the AIMD trajectories, ionic conductivities of Li at temperatures in the range between 600 and 1100 K are calculated, which gives a fitted activation energy of 0.20 eV. The extrapolated ionic conductivity at 300 K is 13.8 mS/cm. NEB calculations suggest that the diffusion barrier along the 1D channel direction and the interchannel directions is 0.09 and 0.31 eV, respectively. The high ionic conductivity and low activation energies predicted here indicate a rapid Li migration in the LaCl₃ lattice with vacancies.

In the experiment, vacancies are introduced by doping high valence ion Ta⁵⁺. After composition optimization, the Li_{0.388}Ta_{0.238}La_{0.475}Cl₃ electrolyte achieves an ionic conductivity of 3.02 mS/cm at 30 °C, with an activation energy of 0.20 eV agreeing with that predicted by AIMD. More experiments

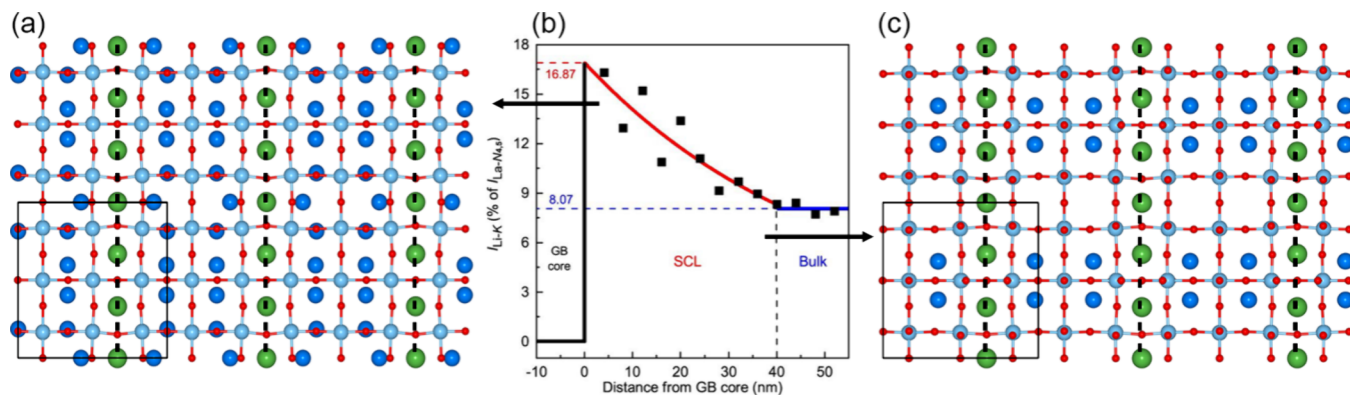


Figure 7. (a) $\text{Li}_{0.66}\text{La}_{0.56}\text{TiO}_3$ as a model in the SCL next to the GB core. (b) EELS characterization of the Li distribution in the SCL. (c) $\text{Li}_{0.33}\text{La}_{0.56}\text{TiO}_3$ as a model in SCL near the bulk region. (b) is reproduced from reference 26. Copyright 2023 Nature Publishing Group.

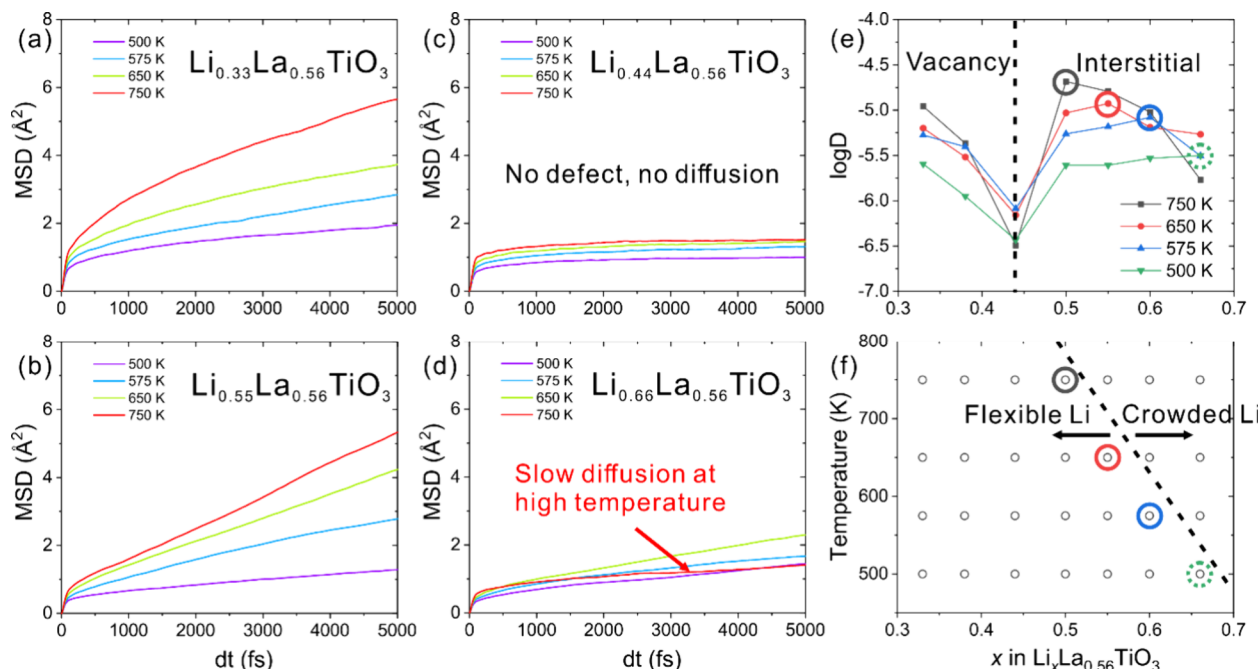


Figure 8. Li MSD in electrolyte (a) $\text{Li}_{0.33}\text{La}_{0.56}\text{TiO}_3$, (b) $\text{Li}_{0.44}\text{La}_{0.56}\text{TiO}_3$, (c) $\text{Li}_{0.55}\text{La}_{0.56}\text{TiO}_3$, and (d) $\text{Li}_{0.66}\text{La}_{0.56}\text{TiO}_3$, (e) Diffusion coefficient as a function of temperature and electrolyte composition. The critical points where the diffusion coefficient starts to decrease are marked by solid circles. Dashed circles indicate the possible position of the critical point. (f) Phase diagram of flexible and crowded Li interstitials. The circles are the same as those in (e). MSD profiles in (a) and (b) are reproduced from reference 26. Copyright 2023 Nature Publishing Group.

suggest that LaCl_3 -based solid electrolytes are quite promising for practical applications of all solid state lithium-metal batteries.

3.3. Ion Diffusion in the Space Charge Layer

Besides conductivity in bulk electrolyte, Li transport through the solid–solid interface is also important for all-solid-state Li batteries. Taking $\text{Li}_{0.33}\text{La}_{0.56}\text{TiO}_3$ as an example, the ionic conductivity of the bulk electrolyte is about 1 mS/cm, while it is only 0.02 mS/cm for grain boundaries (GBs).²⁷ The concept of SCL is commonly accepted to understand the extremely low ionic conductivity.^{50–52} It is suggested that the GB core is positively charged, forming a SCL. This SCL repels positively charged Li ions, resulting in a Li-deficient region.^{53,54} However, recent TEM and EELS observations suggest a different picture. Instead of a Li-deficient region, the SCL near the GB in $\text{Li}_{0.33}\text{La}_{0.56}\text{TiO}_3$ contains more Li than the bulk region (Figure 7).²⁶ The Li concentration gradually decreases

from the GB core to the bulk region, and the maximal Li concentration in SCL can be two times as large as that in the bulk region. Then, there are follow-up questions: How mobile are those Li interstitials? Are they the origin of the low ionic conductivity of the grain boundary?

To answer these questions, AIMD simulations are performed for the solid electrolyte $\text{Li}_x\text{La}_{0.56}\text{TiO}_3$. In the SCL, composition x is in the range of 0.33–0.66 depending on the distance to the GB core. Different compositions are chosen for MD simulations at 500 and 750 K. Two examples are shown in Figure 7. With the increase of x , the defect type in the SCL changes from vacancy to interstitial. As shown in Figure 8, MSDs for systems with vacancies ($\text{Li}_{0.33}\text{La}_{0.56}\text{TiO}_3$) are similar to those of interstitial systems ($\text{Li}_{0.55}\text{La}_{0.56}\text{TiO}_3$), which indicates that the mobility of the Li interstitial is close to that of the Li vacancy. No diffusion event is observed in $\text{Li}_{0.44}\text{La}_{0.56}\text{TiO}_3$ since there is no free defect. Note that $\text{Li}_{0.44}\text{La}_{0.56}\text{TiO}_3$ contains excess Li compared to the bulk phase,

and it only exists in the SCL. For bulk electrolyte without intrinsic defects, the composition is $\text{Li}_{0.5}\text{La}_{0.5}\text{TiO}_3$, which has a low ionic conductivity in experiment.⁵⁵ Since the concentration of Li gradually decreases from the GB core ($\text{Li}_{0.66}\text{La}_{0.56}\text{TiO}_3$) to the bulk region ($\text{Li}_{0.33}\text{La}_{0.56}\text{TiO}_3$) continuously (Figure 7b), a region with the composition close to $\text{Li}_{0.44}\text{La}_{0.56}\text{TiO}_3$ exists in the SCL. This may make an important contribution to the low ionic conductivity in the SCL. Besides this defect-deficient region in the SCL, the GB cores also have a detrimental impact on ion transport, which is another potential origin of the low ionic conductivity of the SCL.⁵⁶⁻⁶⁰

The MSD for $\text{Li}_{0.66}\text{La}_{0.56}\text{TiO}_3$ increases more slowly at 750 K than at 500 or 650 K (Figure 8d). Such an anomalous phenomenon is induced by the saturation of Li interstitials. This is an important difference between vacancies and interstitials. When the concentration of Li interstitials is too high, they can be in a crowded state with a lower ionic conductivity. Such a decrease in Li mobility is clearly shown in Figure 8e, with the turning points marked by solid circles. When temperature is higher, it is easier for Li interstitials to be in a crowded state. As a result, the Li concentration x of the turning point changes from 0.60, 0.55, to 0.50 at temperatures from 575, 650, to 750 K. By connecting these points in the 2D grids of temperature and Li concentration, a boundary between flexible Li and crowded Li can be drawn (Figure 8f). The unusual decrease of Li mobility with the increase of temperature is simply a result of crossing this boundary from the flexible Li side to the crowded Li side.

4. PROPERTIES BEYOND IONIC CONDUCTIVITY

Besides the ionic conductivity, other properties, including the electrochemical stability and the compatibility with the reactive electrode, are also important for the practical application of solid-state electrolytes in batteries. Similar to ionic conductivity, computational techniques also play an important role in the investigation of those properties. The HOMO/LUMO (VBM/CBM) and lithium grand potential phase diagram methods are first introduced to evaluate the electrochemical stability. Then, compatibility with the electrode is addressed.

4.1. Electrochemical Stability

The electrochemical window is widely used as a parameter to characterize the electrochemical stability. Generally, inorganic solid electrolytes should be a good insulator of electronic charge and have wide electrochemical windows. However, electrolyte decomposition induced by the highly reactive lithium electrode is ubiquitous. For example, the inorganic solid electrolyte $\text{Li}_{1+x}\text{Al}_x\text{Ti}_{2-x}(\text{PO}_4)_3$ (LATP) has a limited electrochemical stability due to the reduction of Ti^{4+} ions.³

On the theoretical side, one common model to estimate the electrochemical window is calculating the energy difference between the highest occupied molecular orbital (HOMO) and the lowest unoccupied molecular orbital (LUMO) of electrolyte molecules. For a crystalline solid electrolyte, the HOMO/LUMO can be replaced by the valence band maximum (VBM) and conduction band minimum (CBM). However, such a model does not include effects of redox reactions and the charged electrode/electrolyte interface. As a result, the electrochemical window predicted based on HOMO/LUMO and VBM/CBM is not very accurate.²⁹ As an example, the mean-absolute-errors of electrochemical windows of 68 solvents predicted by the HOMO/LUMO differences reach

3.25 eV compared to experimental values.²⁸ For liquid electrolytes, the accuracy of the electrochemical window prediction can be improved via considering the solvation energy and structure reorganization energy of solvent molecules.

The electrochemical stability of solid electrolytes can also be evaluated by calculating the lithium grand potential phase diagram from first principles.³⁰⁻³² If only the thermodynamic stability is of interest, a phase diagram can be constructed by determining the convex hull³³ of the normalized energy per atom of all possible phases. Some information on these possible phases can be found in the Material Project.³⁴ As an example, the quaternary phase diagram of the Li-Ta-P-O system is shown in Figure 9a, which suggests that LiTa_2PO_8 is

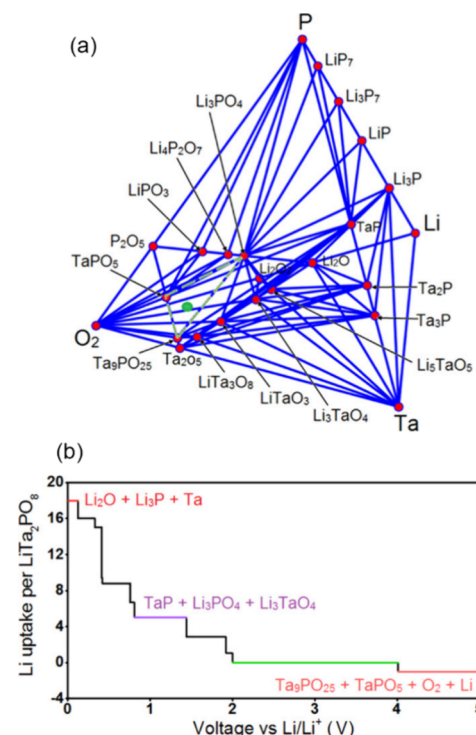


Figure 9. (a) Li-Ta-P-O phase diagram. Red points represent stable phases. LiTa_2PO_8 marked by a green point is metastable. (b) Li uptake against voltage vs Li/Li^+ . The stable electrochemical window of LiTa_2PO_8 is colored by green. Reproduced with permission from reference 22. Copyright 2019 American Chemical Society.

not thermodynamically stable and prefers to decompose into $\text{Ta}_9\text{PO}_{25}$, Li_3PO_4 , and TaPO_5 phases. However, it does not necessarily suggest that the LiTa_2PO_8 material cannot exist in reality since its hull energy is very small.²²

For electrochemical stability, we consider the solid electrolyte coupled with a reservoir of lithium, and a grand potential can be defined as

$$\varphi = E - \mu_{\text{Li}} N_{\text{Li}} \quad (6)$$

where E , μ_{Li} , and N_{Li} are the internal energy, Li chemical potential, and the numbers of Li ions, respectively. Referring to the energy of the Li metal (μ_{Li}^0), the Li chemical potential μ_{Li} is given by minus voltage. Therefore, based on the grand potential, the stability of electrolyte at different voltages can be evaluated, and the electrochemical window can be estimated. As an example, the electrochemical window of LiTa_2PO_8 is estimated to be 2.01–4.01 V (Figure 9b). Such a window is

relatively wide compared to other solid electrolytes such as $\text{Li}_{10}\text{GeP}_2\text{S}_{12}$ ³¹ and $\text{Li}_7\text{P}_3\text{S}_{11}$.³⁵ Similar electrochemical stability analysis can also be performed for Li_3OBr electrolyte.⁷

4.2. Compatibility with Electrode

The compatibility between the solid electrolyte and Li-metal electrode is determined by the properties of the electrode/electrolyte interface. A uniform and stable interface is essential for good electrochemical performance of Li-ion batteries, such as stable cycling performance, low interfacial resistance, and high Coulombic efficiency. Generally, the high intrinsic stiffness of inorganic solid electrolytes suppresses the growth of Li dendrites. However, there can still be compatibility issues limiting the practical application of solid electrolytes, such as poor wettability, high interfacial resistance, low chemical stability, and structural fragmentation induced by volume change of the electrode during the charging and discharging processes.³

To stabilize the reactive Li-metal electrode, a solid electrolyte interphase (SEI) with multiple components forms spontaneously between the electrode and the electrolyte. The failure of the battery follows cycles of Li transportation through the charged electrode/SEI/electrolyte interface. From a theoretical point of view, such a complex process can be separated into different steps and should be studied using different simulation techniques at different scales.^{44,45} Ab initio simulations can be employed to investigate the adsorption and decomposition of a single molecule on the Li electrode surface.³⁶ The electrode/SEI/electrolyte interface and the formation of SEI structures can be simulated by density functional tight binding (DFTB)³⁷ or reactive force field-based MD.^{38,39} Diffusion of ions can also be simulated using MD.⁴⁰ Continuum models without atomic details may be required to study the growth of Li dendrite.^{19,20,41} Machine learning is a powerful tool to reach a good balance between accuracy and efficiency in such multiscale simulations.^{42,43} More details of these simulation techniques are included in the *Supporting Information*.

5. SUMMARY AND OUTLOOK

In this Account, we summarize our recent progress in the theoretical design of solid electrolyte materials. It is demonstrated that different simulation techniques can be used to explore the solid electrolyte properties, including ionic conductivity, electrochemical stability, and electrode/electrolyte compatibility. Based on AIMD simulations, the ionic conductivity of the bulk electrolyte can be predicted. We propose enhancing the ionic conductivity via point defect and diffusion pathway engineering. In Li_3OX ($\text{X} = \text{Cl}, \text{Br}$) based electrolyte, the concentration of vacancy and interstitial defects can be effectively increased by adopting proper crystal structure or by introducing a well-selected charge compensating doping element. In LaCl_3 based electrolyte, a 3D diffusion pathway can be built by connecting intrinsic 1D ion channels via introducing La vacancies. Besides the ionic conductivity of the bulk electrolyte, the Li mobility in SCL is also investigated. With the decrease of Li concentration from the interface to the bulk region in the SCL, a defect depletion region with low ionic conductivity is identified. A Li crowding induced Li mobility decrease with the increase of temperature is also found.

Looking forward, though the properties of inorganic solid electrolytes can be investigated by simulation techniques at

multiple scales, the reliability of connection between different scales and between simulation and experiment is still challenging. With atomistic simulations, the size of the system is limited by the high computational cost. If machine learning and quantum computing techniques can make the atomistic simulation of very large systems affordable, there will be new possibilities for theoretical studies of solid electrolytes. For example, a complete SCL structure with the charged electrode/electrolyte interface can be explicitly simulated, which will predict an accurate electrical field and electrode potential. Then the structure evolution with the influence of accurate electrical field, such as the formation of multi-component SEI structure, the Li deposition, and stripping processes on the charged electrode/SEI/electrolyte interface, can be directly simulated at an atomistic scale.

■ ASSOCIATED CONTENT

SI Supporting Information

The Supporting Information is available free of charge at <https://pubs.acs.org/doi/10.1021/accountsrmr.3c00223>.

Step-by-step procedure to get a profile of Li uptake per formula unit versus voltage; AIMD simulation of a charged electrode/electrolyte interface; and theoretical techniques to simulate a solid electrode/electrolyte interface (PDF)

■ AUTHOR INFORMATION

Corresponding Author

Zhenyu Li – Key Laboratory of Precision and Intelligent Chemistry, University of Science and Technology of China, Hefei, Anhui 230026, China;  orcid.org/0000-0003-2112-9834; Email: zyli@ustc.edu.cn

Author

Jiale Ma – Key Laboratory of Precision and Intelligent Chemistry, University of Science and Technology of China, Hefei, Anhui 230026, China;  orcid.org/0000-0002-3776-2506

Complete contact information is available at: <https://pubs.acs.org/10.1021/accountsrmr.3c00223>

Notes

The authors declare no competing financial interest.

Biographies

Jiale Ma is an associate researcher at the University of Science and Technology of China. He received his B.E. and Ph.D. degrees in materials science from Dalian University of Technology and City University of Hong Kong in 2013 and 2018, respectively. He is interested in the electrical double layer structure at a charged interface and diffusion mechanism of Li ions in solid electrolyte.

Zhenyu Li is a professor of chemistry at University of Science and Technology of China and the director of the Key Laboratory of Precision and Intelligent Chemistry. He received his Ph.D. degree in physical chemistry from University of Science and Technology of China in 2004. His research interests focus on developing and applying new methods to study microscale mechanisms and properties of materials.

ACKNOWLEDGMENTS

This work is supported by National Natural Science Foundation of China (22393913, 22303094) and the Strategic Priority Research Program of the Chinese Academy of Sciences (XDB0450101).

REFERENCES

- (1) Cheng, X. B.; Zhang, R.; Zhao, C. Z.; Zhang, Q. Toward Safe Lithium Metal Anode in Rechargeable Batteries: A Review. *Chem. Rev.* **2017**, *117*, 10403–10473.
- (2) Lin, D.; Liu, Y.; Cui, Y. Reviving the Lithium Metal Anode for High-Energy Batteries. *Nat. Nanotechnol.* **2017**, *12*, 194–206.
- (3) Manthiram, A.; Yu, X.; Wang, S. Lithium Battery Chemistries Enabled by Solid-State Electrolytes. *Nat. Rev. Mater.* **2017**, *2*, 16103.
- (4) Famprikis, T.; Canepa, P.; Dawson, J. A.; Islam, M. S.; Masquelier, C. Fundamentals of Inorganic Solid-State Electrolytes for Batteries. *Nat. Mater.* **2019**, *18*, 1278–1291.
- (5) Chae, O. B.; Lucht, B. L. Interfacial Issues and Modification of Solid Electrolyte Interphase for Li Metal Anode in Liquid and Solid Electrolytes. *Adv. Energy Mater.* **2023**, *13*, 2203791.
- (6) Yin, Y.-C.; Yang, J.-T.; Luo, J.-D.; Lu, G.-X.; Huang, Z.; Wang, J.-P.; Li, P.; Li, F.; Wu, Y.-C.; Tian, T.; Meng, Y.-F.; Mo, H.-S.; Song, Y.-H.; Yang, J.-N.; Feng, L.-Z.; Ma, T.; Wen, W.; Gong, K.; Wang, L.-J.; Ju, H.-X.; Xiao, Y.; Li, Z.; Tao, X.; Yao, H.-B. A LaCl_3 -Based Lithium Superionic Conductor Compatible with Lithium Metal. *Nature* **2023**, *616*, 77–83.
- (7) Hussain, F.; Li, P.; Li, Z.; Yang, J. Ion Conductivity Enhancement in Anti-Spinel Li_3OBr with Intrinsic Vacancies. *Adv. Theory Simulations* **2019**, *2*, 1800138.
- (8) Li, P.; Hussain, F.; Cui, P.; Li, Z.; Yang, J. Boosting Ionic Conductivity in Antiperovskite Li_3OCl via Defect Engineering: Interstitial versus Vacancy. *Phys. Rev. Mater.* **2019**, *3*, 115402.
- (9) Chen, C.; Du, J. Lithium Ion Diffusion Mechanism in Lithium Lanthanum Titanate Solid-State Electrolytes from Atomistic Simulations. *J. Am. Ceram. Soc.* **2015**, *98*, 534–542.
- (10) He, X.; Zhu, Y.; Mo, Y. Origin of Fast Ion Diffusion in Super-Ionic Conductors. *Nat. Commun.* **2017**, *8*, 15893.
- (11) Emly, A.; Kioupakis, E.; Van Der Ven, A. Phase Stability and Transport Mechanisms in Antiperovskite Li_3OCl and Li_3OBr Superionic Conductors. *Chem. Mater.* **2013**, *25*, 4663–4670.
- (12) Deng, Y.; Eames, C.; Nguyen, L. H. B.; Pecher, O.; Griffith, K. J.; Courty, M.; Fleutot, B.; Chotard, J. N.; Grey, C. P.; Islam, M. S.; Masquelier, C. Crystal Structures, Local Atomic Environments, and Ion Diffusion Mechanisms of Scandium-Substituted Sodium Superionic Conductor (NASICON) Solid Electrolytes. *Chem. Mater.* **2018**, *30*, 2618–2630.
- (13) Malik, R.; Burch, D.; Bazant, M.; Ceder, G. Particle Size Dependence of the Ionic Diffusivity. *Nano Lett.* **2010**, *10*, 4123–4127.
- (14) Jay, E. E.; Rushton, M. J. D.; Chroneos, A.; Grimes, R. W.; Kilner, J. A. Genetics of Superionic Conductivity in Lithium Lanthanum Titanates. *Phys. Chem. Chem. Phys.* **2015**, *17*, 178–183.
- (15) Jäckle, M.; Helmbrecht, K.; Smits, M.; Stottmeister, D.; Groß, A. Self-Diffusion Barriers: Possible Descriptors for Dendrite Growth in Batteries? *Energy Environ. Sci.* **2018**, *11*, 3400–3407.
- (16) Jäckle, M.; Groß, A. Influence of Electric Fields on Metal Self-Diffusion Barriers and Its Consequences on Dendrite Growth in Batteries. *J. Chem. Phys.* **2019**, *151*, 234707.
- (17) Byun, K.; Saha, J. K.; Jang, J. Role of a Solid-Electrolyte Interphase in the Dendritic Electrodeposition of Lithium: A Brownian Dynamics Simulation Study. *J. Phys. Chem. C* **2020**, *124* (17), 9134–9141.
- (18) Kamphaus, E. P.; Hight, K.; Dermott, M.; Balbuena, P. B. Model Systems for Screening and Investigation of Lithium Metal Electrode Chemistry and Dendrite Formation. *Phys. Chem. Chem. Phys.* **2020**, *22*, 575–588.
- (19) Chen, L.; Zhang, H. W.; Liang, L. Y.; Liu, Z.; Qi, Y.; Lu, P.; Chen, J.; Chen, L. Q. Modulation of Dendritic Patterns during Electrodeposition: A Nonlinear Phase-Field Model. *J. Power Sources* **2015**, *300*, 376–385.
- (20) Hong, Z.; Viswanathan, V. Phase-Field Simulations of Lithium Dendrite Growth with Open-Source Software. *ACS Energy Lett.* **2018**, *3*, 1737–1743.
- (21) Henkelman, G.; Uberuaga, B. P.; Jónsson, H. A Climbing Image Nudged Elastic Band Method for Finding Saddle Points and Minimum Energy Paths. *J. Chem. Phys.* **2000**, *113*, 9901–9904.
- (22) Hussain, F.; Li, P.; Li, Z. Theoretical Insights into Li-Ion Transport in LiTa_2PO_8 . *J. Phys. Chem. C* **2019**, *123*, 19282–19287.
- (23) Li, P.; Zeng, X.; Li, Z. Understanding High-Temperature Chemical Reactions on Metal Surfaces: A Case Study on Equilibrium Concentration and Diffusivity of C_xH_y on a Cu(111) Surface. *JACS Au* **2022**, *2* (2), 443–452.
- (24) Tilley, R. J. D. Defects and Diffusion. In *Defects in Solids*; John Wiley and Sons Inc.: Hoboken, NJ, 2008; pp 205–250.
- (25) Kim, J.; Kim, J.; Avdeev, M.; Yun, H.; Kim, S. J. LiTa_2PO_8 : A Fast Lithium-Ion Conductor with New Framework Structure. *J. Mater. Chem. A* **2018**, *6*, 22478–22482.
- (26) Gu, Z.; Ma, J.; Zhu, F.; Liu, T.; Wang, K.; Nan, C. W.; Li, Z.; Ma, C. Atomic-Scale Study Clarifying the Role of Space-Charge Layers in a Li-Ion-Conducting Solid Electrolyte. *Nat. Commun.* **2023**, *14*, 1632.
- (27) Inaguma, Y.; Liquan, C.; Itoh, M.; Nakamura, T.; Uchida, T.; Ikuta, H.; Wakihara, M. High Ionic Conductivity in Lithium Lanthanum Titanate. *Solid State Commun.* **1993**, *86*, 689–693.
- (28) Wang, D.; He, T.; Wang, A.; Guo, K.; Avdeev, M.; Ouyang, C.; Chen, L.; Shi, S. A Thermodynamic Cycle-Based Electrochemical Windows Database of 308 Electrolyte Solvents for Rechargeable Batteries. *Adv. Funct. Mater.* **2023**, *33*, 2212342.
- (29) Peljo, P.; Girault, H. H. Electrochemical Potential Window of Battery Electrolytes: The HOMO-LUMO Misconception. *Energy Environ. Sci.* **2018**, *11*, 2306–2309.
- (30) Ong, S. P.; Wang, L.; Kang, B.; Ceder, G. Li-Fe-P-O₂ Phase Diagram from First Principles Calculations. *Chem. Mater.* **2008**, *20*, 1798–1807.
- (31) Mo, Y.; Ong, S. P.; Ceder, G. First Principles Study of the $\text{Li}_{10}\text{GeP}_2\text{S}_{12}$ Lithium Super Ionic Conductor Material. *Chem. Mater.* **2012**, *24*, 15–17.
- (32) Ong, S. P.; Richards, W. D.; Jain, A.; Hautier, G.; Kocher, M.; Cholia, S.; Gunter, D.; Chevrier, V. L.; Persson, K. A.; Ceder, G. Python Materials Genomics (Pymatgen): A Robust, Open-Source Python Library for Materials Analysis. *Comput. Mater. Sci.* **2013**, *68*, 314–319.
- (33) Barber, C. B.; Dobkin, D. P.; Huhdanpaa, H. The Quickhull Algorithm for Convex Hulls. *ACM Trans. Math. Softw.* **1996**, *22*, 469–483.
- (34) Jain, A.; Ong, S. P.; Hautier, G.; Chen, W.; Richards, W. D.; Dacek, S.; Cholia, S.; Gunter, D.; Skinner, D.; Ceder, G.; Persson, K. A. Commentary: The Materials Project: A Materials Genome Approach to Accelerating Materials Innovation. *APL Mater.* **2013**, *1*, 011002.
- (35) Chu, I. H.; Nguyen, H.; Hy, S.; Lin, Y. C.; Wang, Z.; Xu, Z.; Deng, Z.; Meng, Y. S.; Ong, S. P. Insights into the Performance Limits of the $\text{Li}_7\text{P}_3\text{S}_{11}$ Superionic Conductor: A Combined First-Principles and Experimental Study. *ACS Appl. Mater. Interfaces* **2016**, *8*, 7843–7853.
- (36) Leung, K.; Qi, Y.; Zavadil, K. R.; Jung, Y. S.; Dillon, A. C.; Cavanagh, A. S.; Lee, S.-H.; George, S. M. Using Atomic Layer Deposition to Hinder Solvent Decomposition in Lithium Ion Batteries: First-Principles Modeling and Experimental Studies. *J. Am. Chem. Soc.* **2011**, *133*, 14741–14754.
- (37) Li, Y.; Leung, K.; Qi, Y. Computational Exploration of the Li-Electrode/Electrolyte Interface in the Presence of a Nanometer Thick Solid-Electrolyte Interphase Layer. *Acc. Chem. Res.* **2016**, *49*, 2363–2370.
- (38) Kim, S. P.; Duin, A. C. T. V.; Shenoy, V. B. Effect of Electrolytes on the Structure and Evolution of the Solid Electrolyte

- Interphase (SEI) in Li-Ion Batteries: A Molecular Dynamics Study. *J. Power Sources* **2011**, *196*, 8590–8597.
- (39) Yun, K. S.; Pai, S. J.; Yeo, B. C.; Lee, K. R.; Kim, S. J.; Han, S. S. Simulation Protocol for Prediction of a Solid-Electrolyte Interphase on the Silicon-Based Anodes of a Lithium-Ion Battery: ReaxFF Reactive Force Field. *J. Phys. Chem. Lett.* **2017**, *8*, 2812–2818.
- (40) Borodin, O.; Ren, X.; Vatamanu, J.; Von Wald Cresce, A.; Knap, J.; Xu, K. Modeling Insight into Battery Electrolyte Electrochemical Stability and Interfacial Structure. *Acc. Chem. Res.* **2017**, *50*, 2886–2894.
- (41) Klinsmann, M.; Rosato, D.; Kamlah, M.; McMeeking, R. M. Modeling Crack Growth during Li Extraction in Storage Particles Using a Fracture Phase Field Approach. *J. Electrochem. Soc.* **2016**, *163*, A102–A118.
- (42) Unke, O. T.; Chmiela, S.; Sauceda, H. E.; Gastegger, M.; Poltavsky, I.; Schütt, K. T.; Tkatchenko, A.; Müller, K. R. Machine Learning Force Fields. *Chem. Rev.* **2021**, *121*, 10142–10186.
- (43) Deringer, V. L.; Caro, M. A.; Csányi, G. Machine Learning Interatomic Potentials as Emerging Tools for Materials Science. *Adv. Mater.* **2019**, *31*, 1902765.
- (44) Takenaka, N.; Bouibes, A.; Yamada, Y.; Nagaoka, M.; Yamada, A. Frontiers in Theoretical Analysis of Solid Electrolyte Interphase Formation Mechanism. *Adv. Mater.* **2021**, *33*, 2100574.
- (45) Diddens, D.; Appiah, W. A.; Mabrouk, Y.; Heuer, A.; Vegge, T.; Bhowmik, A. Modeling the Solid Electrolyte Interphase: Machine Learning as a Game Changer? *Adv. Mater. Interfaces* **2022**, *9*, 2101734.
- (46) Zhao, Y.; Daemen, L. L. Superionic Conductivity in Lithium-Rich Anti-Perovskites. *J. Am. Chem. Soc.* **2012**, *134*, 15042–15047.
- (47) Zhang, Y.; Zhao, Y.; Chen, C. Ab Initio Study of the Stabilities of and Mechanism of Superionic Transport in Lithium-Rich Antiperovskites. *Phys. Rev. B* **2013**, *87*, 134303.
- (48) Kröger, F. A.; Vink, H. J. Relations between the Concentrations of Imperfections in Crystalline Solids. *Solid State Phys.* **1956**, *3*, 307–435.
- (49) He, X.; Bai, Q.; Liu, Y.; Nolan, A. M.; Ling, C.; Mo, Y. Crystal Structural Framework of Lithium Super-Ionic Conductors. *Adv. Energy Mater.* **2019**, *9*, 1902078.
- (50) Zhang, J.; Zheng, C.; Li, L.; Xia, Y.; Huang, H.; Gan, Y.; Liang, C.; He, X.; Tao, X.; Zhang, W. Unraveling the Intra and Intercycle Interfacial Evolution of $\text{Li}_6\text{PS}_3\text{Cl}$ -Based All-Solid-State Lithium Batteries. *Adv. Energy Mater.* **2020**, *10*, 1903311.
- (51) Wang, L.; Xie, R.; Chen, B.; Yu, X.; Ma, J.; Li, C.; Hu, Z.; Sun, X.; Xu, C.; Dong, S.; Chan, T. S.; Luo, J.; Cui, G.; Chen, L. In-Situ Visualization of the Space-Charge-Layer Effect on Interfacial Lithium-Ion Transport in All-Solid-State Batteries. *Nat. Commun.* **2020**, *11*, 5889.
- (52) Cheng, Z.; Liu, M.; Ganapathy, S.; Li, C.; Li, Z.; Zhang, X.; He, P.; Zhou, H.; Wagemaker, M. Revealing the Impact of Space-Charge Layers on the Li-Ion Transport in All-Solid-State Batteries. *Joule* **2020**, *4*, 1311–1323.
- (53) Wu, J. F.; Guo, X. Origin of the Low Grain Boundary Conductivity in Lithium Ion Conducting Perovskites: $\text{Li}_{3x}\text{La}_{0.67-x}\text{TiO}_3$. *Phys. Chem. Chem. Phys.* **2017**, *19*, 5880–5887.
- (54) Sasano, S.; Ishikawa, R.; Sánchez-Santolino, G.; Ohta, H.; Shibata, N.; Ikuhara, Y. Atomistic Origin of Li-Ion Conductivity Reduction at $(\text{Li}_{3x}\text{La}_{2/3-x})\text{TiO}_3$ Grain Boundary. *Nano Lett.* **2021**, *21*, 6282–6288.
- (55) Inaguma, Y.; Itoh, M. Influences of Carrier Concentration and Site Percolation on Lithium Ion Conductivity in Perovskite-Type Oxides. *Solid State Ionics* **1996**, *86–88*, 257–260.
- (56) Heo, T. W.; Grieder, A.; Wang, B.; Wood, M.; Hsu, T.; Akhade, S. A.; Wan, L. F.; Chen, L.-Q.; Adelstein, N.; Wood, B. C. Microstructural Impacts on Ionic Conductivity of Oxide Solid Electrolytes from a Combined Atomistic-Mesoscale Approach. *NPJ Comput. Mater.* **2021**, *7*, 214.
- (57) Golov, A.; Carrasco, J. Enhancing First-Principles Simulations of Complex Solid-State Ion Conductors Using Topological Analysis of Procrystal Electron Density. *NPJ. Comput. Mater.* **2022**, *8*, 187.
- (58) Dawson, J. A. Going against the Grain: Atomistic Modeling of Grain Boundaries in Solid Electrolytes for Solid-State Batteries. *ACS Materials Au* **2024**, *4*, 1–13.
- (59) Dawson, J. A.; Canepa, P.; Famprakis, T.; Masquelier, C.; Islam, M. S. Atomic-Scale Influence of Grain Boundaries on Li-Ion Conduction in Solid Electrolytes for All-Solid-State Batteries. *J. Am. Chem. Soc.* **2018**, *140*, 362–368.
- (60) Quirk, J. A.; Dawson, J. A. Design Principles for Grain Boundaries in Solid-State Lithium-Ion Conductors. *Adv. Energy Mater.* **2023**, *13*, 2301114.